BIOCHEMISTRY
including biophysical chemistry & molecular biology

Article

Thiol and sulfenic acid oxidation of AhpE, the one-cysteine peroxiredoxin from Mycobacterium tuberculosis: kinetics, acidity constants and conformational dynamics

Martín Hugo, Lucía Turell, Bruno Manta, Horacio Botti, Gisele Monteiro, Luis Eduardo S. Netto, Beatriz Alvarez, Rafael Radi, and Madia Trujillo

Biochemistry, **Just Accepted Manuscript** • DOI: 10.1021/bi901221s • Publication Date (Web): 08 September 2009

Thiol and sulfenic acid oxidation of AhpE, the one-cysteine peroxiredoxin from *Mycobacterium tuberculosis*: kinetics, acidity constants and conformational dynamics[†]

Martín Hugo,[‡,§] Lucía Turell,[‖,§] Bruno Manta,[⊥,§] Horacio Botti,[⊥,§] Gisele Monteiro,[#] Luis E. S. Netto,[#] Beatriz Alvarez,[‖,§] Rafael Radi,[‡,§] Madia Trujillo*[,‡,§]

[‡] Departamento de Bioquímica, Facultad de Medicina, Universidad de la República, Montevideo, Uruguay

[§] Center for Free Radical and Biomedical Research, Facultad de Medicina, Universidad de la República, Montevideo, Uruguay

[‖] Instituto de Química Biológica, Facultad de Ciencias, Universidad de la República, Montevideo, Uruguay

[⊥] Institut Pasteur de Montevideo, Montevideo, Uruguay

[#] Departamento de Biologia, Instituto de Biociências, Universidade de São Paulo, São Paulo, Brazil

* To whom correspondence should be addressed: Dr. Madia Trujillo, Departamento de Bioquímica and Center for Free Radical and Biomedical Research, Facultad de Medicina, Universidad de la República, General Flores 2125, 11800 Montevideo, Uruguay. E-mail: madiat@fmed.edu.uy. Telephone: (5982)9249561. Fax: (5982)9249563.

Running title: *Mycobacterium tuberculosis* AhpE oxidation and overoxidation

† This work was supported by grants from Programa de Desarrollo Tecnológico (PDT 079), Ministerio de Educación y Cultura, Uruguay, to MT and BA; from Howard Hughes Medical Institute and International Centre of Genetic Engineering and Biotechnology to RR; from FAPESP and INCT de Processos Redox em Biomedicina, Brazil to LESN and GM. MH, BM, LT and HB were supported by fellowships from PEDECIBA-ANII, Uruguay.

[1]

[1] *Abbreviations:* C_P, peroxidatic cysteine; DTNB, 5,5'-dithio-bis(2-nitrobenzoate); dtpa, diethylenetriaminepentaacetic acid; DTT, dithiothreitol; GSH, glutathione; HRP, horseradish peroxidase; LiP, lignine peroxidase; *Mt*AhpE, *Mycobacterium tuberculosis* alkyl hydroperoxide reductase E; NAC, N-acetylcysteine; NEM, N-ethylmaleimide; Prx, peroxiredoxin; TNB, 5-thio-2-nitrobenzoate.

Abstract

Drug resistance and virulence of *Mycobacterium tuberculosis* are partially related to the pathogen's antioxidant systems. Peroxide detoxification in this bacterium is achieved by the heme-containing catalase peroxidase, and different two-cysteine peroxiredoxins. *M. tuberculosis* genome also codifies for a putative one-cysteine peroxiredoxin, alkyl hydroperoxide reductase E (*Mt*AhpE). Its expression was previously demonstrated at a transcriptional level, and the crystallographic structure of the recombinant protein was resolved under reduced and oxidized states. Herein, we report that the conformation of *Mt*AhpE changed depending on its single cysteine redox state, as reflected by different tryptophan fluorescence properties and changes in quaternary structure. Dynamics of fluorescence changes, complemented by competition kinetic assays, were used to perform protein functional studies. *Mt*AhpE reduced peroxynitrite two orders of magnitude faster than hydrogen peroxide (1.9×10^7 $M^{-1}s^{-1}$ *vs* 8.2×10^4 $M^{-1}s^{-1}$ at pH 7.4 and 25°C, respectively). The latter also caused cysteine overoxidation to sulfinic acid, but at much slower rate (40 $M^{-1}s^{-1}$). The pK_a of the thiol in the reduced enzyme was 5.2, more than one unit lower than that of the sulfenic acid in the oxidized enzyme. The pH profile of hydrogen peroxide-mediated thiol and sulfenic acid oxidations indicated thiolate and sulfenate as the reacting species. The formation of sulfenic acid as well as the catalytic peroxidase activity of *Mt*AhpE were demonstrated using the artificial reducing substrate thionitrobenzoate. Taken together our results indicate that *Mt*AhpE is a relevant component in the antioxidant repertoire of *Mycobacterium tuberculosis* probably involved in peroxide, and specially peroxynitrite detoxification.

Tuberculosis (TB) is a serious, often lethal infectious disease caused by *Mycobacterium tuberculosis*, which affects about one third of the human population. Multidrug resistance TB is an emerging problem of great public health concern worldwide, making new drug development a priority (*1*). This bacterium is able to live and proliferate within the phagosomes of activated macrophages, where it is exposed to a strong oxidative stress (*2*) that includes hydrogen peroxide (H_2O_2) and peroxynitrite[2] production. Reactive oxygen and nitrogen species are cytotoxic (*3-5*), and several lines of evidence indicate their role in the control of *M. tuberculosis* infection (*5-7*). Thus, the mechanisms that allow the pathogen to cope with these species constitute an active field of investigation (*2, 8, 9*).

The antioxidant defense in *M. tuberculosis* is unusual in many aspects. While *M. tuberculosis* lacks the typical glutathione system, it contains millimolar concentrations of mycothiol [2-(N-acetylcysteinyl)amido-2-deoxy-alpha-D-glucopyranosyl-myo-inositol](*10*), mycothiol reductase (*11*) and different thiol disulfide oxidoreductases (*12, 13*). It also contains catalase peroxidase, a heme-dependent peroxidase, that reduces different peroxides including peroxynitrite, and is responsible for the activation of the first line anti-tuberculosis prodrug isoniazid (*14, 15*). As expected, mutations of *katG* result in resistance to this drug (*16*) and interestingly, infective forms of *katG* mutants show increased expression of alkyl hydroperoxide reductase C (AhpC) (*17*), a member of the peroxiredoxin (Prx) family. *M. tuberculosis* also expresses thioredoxin peroxidase (TPx) another two-Cys Prx, which is known to react rapidly with peroxynitrite (*9*) and has been recently proved to be an important virulence factor in cellular and animal models of TB (*18*). In addition, *M. tuberculosis* genome codifies for

[2]The term peroxynitrite is used to refer to the sum of peroxynitrite anion ($ONOO^-$) and peroxynitrous acid (ONOOH) unless specified. IUPAC recommended names for $ONOO^-$ and ONOOH are oxoperoxonitrate(1-) and hydrogen oxoperoxonitrate, respectively.

other three Prxs (*19*). Among them, the hypothetical bacterioferritin comigratory proteins have proved to be important for survival under oxidative stress conditions in other organisms (*20, 21*). Finally, a gene for a putative one-Cys Prx, alkyl hydroperoxide reductase E (AhpE, annotated as Rv2238c), has also been identified in *M. tuberculsosis* and is highly conserved among many other Mycobacteria (*19, 22*). The regulated expression of *Mt*AhpE has been reported at a transcriptional level (*23*) and the crystallographic structures of the recombinant protein under reduced and oxidized states have been determined (*24*). In solution, the enzyme was reported to be present as a mixture of dimeric and octameric forms, but redox state-dependent changes in its quaternary structure, as observed for other Prxs (*25*), have not been previously investigated. The functional properties of *Mt*AhpE have not been addressed so far. MtAhpE protein contains a single cysteine residue (Cys45) that is predicted to be the peroxidatic cysteine (C_p), since it is located in a typical **P**XXX**T**XX**C** motif, well conserved in the amino acidic sequence of Prx active sites. Moreover, structural data on the recombinant enzyme shows that an arginine residue (Arg116) interacts by hydrogen bonding with Cys45 ($\sim$ 3.5 Å distant) allowing thiolate stabilization, another conserved featured among different Prxs (*26*) .

During the oxidative part of the catalytic cycle of Prxs the thiolate in C_P ($Prx\text{-}S^-$) reduces peroxide substrates such as hydrogen peroxide (H_2O_2), peroxynitrous acid (ONOOH) or organic peroxides (ROOH) to water, nitrite or alcohols (ROH), respectively, in a two-electron oxidation process that leads to sulfenic acid (Prx-SOH) formation:

$$Prx\text{-}S^- + \begin{matrix} H_2O_2 \\ ONOOH \\ ROOH \end{matrix} \longrightarrow Prx\text{-}SOH + \begin{matrix} HO^- \\ NO_2^- \\ RO^- \end{matrix} \qquad (1)$$

In the crystal structure of the oxidized form of *Mt*AhpE, Cys45 was oxidized to a stable sulfenic acid (*24*), as previously reported for the human one-Cys Prx (*27*). In contrast to most two-Cys Prxs (*28*), the reducing step of one-Cys Prxs is still unclear. (*29-33*).

Alternatively, and in the presence of high peroxide concentrations, sulfenic acid in Prxs can be overoxidized to sulfinic acid (Prx-SO_2H), through the reaction with a second molecule of oxidizing substrate, in a process that results in enzyme inactivation

$$\text{Prx-SOH} + \text{ROOH} \rightarrow \text{Prx-SO}_2\text{H} + \text{ROH} \qquad (2)$$

Overoxidation of the mammalian one-Cys Prx has been detected in cellular systems (*34*). There is just one estimation for the second-order rate constant of the reaction in Eq. 2, which is related to mammalian Prx 1 overoxidation by H_2O_2 (57 $M^{-1}s^{-1}$ at physiological pH (*35*) estimated from (*36*)). The mechanism of the reaction, including the reacting species (RSO^- *vs* RSOH) as well as the pK_a of Prxs sulfenic acids, which may affect the rate of the reaction at physiological pH, is far from being resolved.

In this work we demonstrate the peroxidatic activity of the putative one-cysteine Prx of *M. tuberculosis*, AhpE. Taking advantage of the different intrinsic fluorescence properties of this enzyme at its different redox states, or by using competition kinetic approaches, we investigated the enzymatic selectivity towards the main peroxide substrates the bacterium may encounter during infection. We performed mechanistic and kinetic studies on enzymatic overoxidation. The pK_a values of the thiol in the reduced enzyme as well as that of the sulfenic acid in the oxidized enzyme were determined. The results obtained add to our knowledge of the peroxide detoxification mechanisms in *M. tuberculosis*, an important issue for understanding the biology of this extremely successful human pathogen.

Materials and methods

Chemicals. Horseradish peroxidase (HRP) and lignine peroxidase (LiP) were obtained from Sigma and Fluka, respectively. Argon (99.5% pure) was from AGA Gas Company, Montevideo, Uruguay. Hydrogen peroxide (H_2O_2) was from Mallinckrodt Chemicals. Peroxynitrite was synthesized from H_2O_2 and nitrous acid as described previously (*37, 38*). Treatment of a stock solution of peroxynitrite with granular manganese dioxide eliminated H_2O_2 remaining from the synthesis. Nitrite contamination was typically less than 30% of peroxynitrite concentration. 5-thio-2-nitrobenzoate (TNB) free of its disulfide, 5,5'-dithio-bis(2-nitrobenzoate) (DTNB), was synthesized as previously described (*39*). All other reagents were obtained from standard commercial sources and used as received.

All experiments were performed in 100 mM sodium phosphate buffer containing 0.1 mM diethylenetriamine-pentaacetic acid (dtpa), pH 7.4 and 25 ºC, unless otherwise indicated.

*Protein expression and purification. Mt*AhpE (TB Database gene name Rv2238c) was expressed in *Escherichia coli* BL21(DE2)pLys (expression vector pDEST17) as a recombinant His-tagged protein and purified as previously described (*24*). The *Mt*AhpE mutant C45S was generated by site-directed mutagenesis using QuikChange Site-Directed Mutagenesis kit (Stratagene) as described by the manufacturer (previously reported in (*31*)), using the following primers:

C45Sfw: 5'CAC GGG CAT CTC ACA GGG CGA GC 3'

C45Srev:5'GCT CGC CCT GTG AGA TGC CCG TG 3'

Peroxide, protein and thiol quantitation. The concentration of H_2O_2 stock solutions was measured at 240 nm ($\varepsilon_{240} = 43.6\ M^{-1}cm^{-1}$) (*40*). Peroxynitrite

concentration was determined at alkaline pH at 302 nm (ε_{302} = 1670 M^{-1} cm^{-1})(*38*). *Mt*AhpE concentration was determined spectrophotometrically at 280 nm, using a molar absorption coefficient of 23950 $M^{-1}cm^{-1}$ calculated according to (*41*), that was in good agreement with protein measurements by the Biuret assay (not shown). Protein thiol content was measured by Ellman´s assay (ε_{412} = 14150 $M^{-1}cm^{-1}$). Recently purified *Mt*AhpE typically contained ~ 0.9 thiols/protein and thiol content diminished with storage (under argon atmosphere, at -80 ºC)[3]. The concentrations of HRP and LiP were determined by their absorption at the Soret band, (ε_{403} = 1.02 x 10^5 M^{-1} cm^{-1} (*42*) and ε_{409} = 1.68 x 10^5 M^{-1} cm^{-1} (*43*), respectively).

Protein thiol reduction and alkylation. *Mt*AhpE was reduced immediately before use by incubation with 1 mM DTT for 30 minutes at 4 ºC. Excess reductant was removed either by gel filtration using a Hitrap column (Amersham Bioscience) and UV-vis detection at 280 nm or, when using small volumes (< 200 µl), by passing the enzyme twice through Micro-biospin 6 chromatography columns (BioRad). Samples were extensively purged with argon once collected. For protein thiol alkylation, previously reduced *Mt*AhpE was incubated with N-ethylmaleimide (NEM) (5 or 10 mM) for 30 minutes at 4 ºC, and excess NEM was removed as described for DTT.

Changes in the intrinsic fluorescence intensity of MtAhpE. Emission spectra (λ_{exc} = 280 or 295 nm) of wild type or C45S enzyme (1.5 µM) were obtained using an Aminco Bowman Series 2 luminescence spectrophotometer.

Size-Exclusion Chromatography. 250 µL of *Mt*AhpE (0.1 mg of protein) under different redox states were resolved on a Superdex 75 10/300 column, preequilibrated with phosphate buffer (20 mM, 150 mM NaCl, pH 7.4, 0.5 mL/min), with UV detection

[3] Due to the rapid reaction of oxidized *Mt*AhpE with TNB (see below), that could result in thiol content underestimation, thiol quantifications were performed in pre-reduced enzyme or in recently purified enzyme.

at 215 and 280 nm and flow rate of 0.5 mL/min at 25 ºC. The column was calibrated with molecular weight standards (Sigma–Aldrich).

Electrophoretic analysis of MtAhpE. SDS-PAGE electrophoresis of reduced and oxidized enzyme under non-reducing conditions were performed using 13 % acrylamide gels (0.2 µg protein per well), that were silver stained for protein detection.

Electrospray Ionization Mass Spectrometry (ESI-MS) analysis. Freshly purified enzyme was incubated with indicated concentrations of NEM (during 30 minutes), DTT or H_2O_2 (during 2 minutes), or with H_2O_2 (during 1 minute) followed by DTT, N-acetylcysteine (NAC) or glutathione (GSH) addition for two additional minutes in the above mentioned buffer, pH 7.4 and 25ºC. Samples were passed twice through Micro-biospin 6 columns equilibrated with H_2O, diluted into 1:1 acetonitrile:H_2O 0.1% acetic acid, pH 4.5 to a final concentration of 1 µM and loaded into a QTRAP 2000 mass spectrometer (Applied Biosystems/MDS Sciex). Positive ion ESI mass spectra were collected using an *m*/*z* range of 700-1700, with ion spray voltage (IS) 5000 V, declustering potential (DP) 60 V, and entrance potential (EP) 10 V. Data acquisition was set to 3 min, and the final mass of *Mt*AhpE was calculated by automatic deconvolution using Analyst 1.4 software.

Kinetics of MtAhpE oxidation and overoxidation studied using a fluorimetric approach. The rate constants of *Mt*AhpE oxidation by H_2O_2 and peroxynitrite (Eq. 1) were determined by taking advantage of the decrease in protein intrinsic fluorescence intensity (λ_{exc} = 280 nm) that occurred upon oxidation. Reduced, NEM-blocked wild type *Mt*AhpE or C45S mutant (*Mt*AhpEC45S), were rapidly mixed with either peroxynitrite or H_2O_2 in excess in an Applied Photophysics SX-17MV stopped-flow spectrophotometer with a mixing time of <2 ms. Although peroxynitrite is an unstable species, it decays with a first order rate constant of 0.27 s^{-1} at pH 7.4 and 25 ºC, much

slower than the reaction with *Mt*AhpE, so that pseudo-first order conditions are maintained over the time course of reaction (<0.1 s). Observed rate constants of fluorescence decrease (k_{obs}) were determined by fitting stopped-flow data to single exponential functions. Second order rate constants for the reaction between pre-reduced enzyme and peroxynitrite or H_2O_2 were obtained from the slope of the plot of k_{obs} *versus* oxidant concentration.

For the determination of the rate constant of oxidized *Mt*AhpE overoxidation by H_2O_2 (Eq. 2), we took advantage of the increase in the enzyme intrinsic fluorescence intensity that occurred when it was treated with a large excess of H_2O_2. Reduced or NEM-blocked wild type *Mt*AhpE (1 μM) was mixed with H_2O_2 (100 – 450 μM) in an Aminco Bowman Series 2 luminescence spectrophotometer, and time courses of fluorescence intensity change (λ_{exc} = 295 nm, λ_{em} = 338 nm) were registered. Second order rate constants were obtained as described above for enzyme oxidation.

The pK_a of both the peroxidatic thiol group in reduced *Mt*AhpE and the sulfenic acid in oxidized *Mt*AhpE were measured by determining the rate constants of H_2O_2-mediated *Mt*AhpE C_P oxidation and overoxidation (Eqs. 1 and 2, respectively) at different pH values. Buffer systems used were sodium phosphate 100 mM plus 0.1 mM dtpa (pHs 5.8-7.8) or sodium acetate buffer 100 mM plus 0.1 mM dtpa (pHs < 5.8), with NaCl additions so as keep ionic strength constant. When analyzing the effect of pH on overoxidation, the reduced enzyme was previously oxidized to sulfenic acid by treatment with equimolar amount of H_2O_2 for 2 minutes at pH 7.4, 25ºC, and then exposed to excess H_2O_2 at the pH of interest. Rate constants for oxidation and overoxidation (k_{app}) were plotted against pH and fitted to:

$$k_{app} = k_2 \frac{K_{AH}}{K_{AH} + [H^+]} \qquad (3)$$

where k_{app} is the observed rate constant for *Mt*AhpE thiol oxidation ($k_{AhpE\text{-}S^-\ app}$) or overoxidation ($k_{AhpE\text{-}SO^-\ app}$) at a given pH value; k_2 represents the maximum rate constants for the reactions at alkaline pH, *i.e.* the pH independent rate constants and K_{AH} is the equilibrium constant for the deprotonation processes, where AH represents either the peroxidatic thiol or the sulfenic acid intermediate.

Kinetics of MtAhpE oxidation studied by a competition approach. The second-order rate constants for the reactions between reduced *Mt*AhpE and H_2O_2 or peroxynitrite were also determined by competition assays as reported previously (*44-47*). HRP was used to determine the rate constant for the reaction between *Mt*AhpE and peroxynitrite, whereas LiP was used for determining that between *Mt*AhpE and H_2O_2. In both cases, the reactions were followed using an Applied Photophysics SX-17MV stopped-flow spectrophotometer.

In the case of peroxynitrite-mediated HRP oxidation, the reaction was followed at 398 nm and HRP-compound I concentration was measured using a $\Delta\varepsilon_{398} = 4.2 \times 10^4$ M^{-1} cm^{-1} (*48*). The rate constant of peroxynitrite-mediated HRP oxidation to compound I was determined as 3×10^6 $M^{-1}s^{-1}$ under the experimental conditions employed herein (data not shown) in agreement with previously published data (*49*). The rate constant of peroxynitrite-mediated *Mt*AhpE oxidation was calculated as previously (*44-47*).

In the case of H_2O_2-mediated LiP oxidation, the reaction was followed at 401 nm (isosbestic point for LiP-compound I and II determined by us, data not shown) and LiP-compound I concentration was determined assuming an equimolar reaction with H_2O_2. The rate constant for H_2O_2-mediated LiP oxidation to compound I was measured as 6.5×10^5 $M^{-1}s^{-1}$ at pH 7.4 and 25ºC (data not shown), in agreement with previously reported values (*43*). The rate constant of H_2O_2-mediated *Mt*AhpE oxidation was calculated as above.

Computer-assisted simulations were performed using GEPASI 3 program (*50, 51*).

Kinetics of MtAhpE reaction with TNB and DTNB. The reactions were studied using a Varian Cary 50 spectrophotometer with a stopped flow accessory (Applied Photophysics RX 2000). Thionitrobenzoate has been previously used to quantify sulfenic acid formed in one-Cys Prxs and human serum albumin upon oxidation (*39, 52*). Herein, the kinetics of *Mt*AhpE reduction by TNB was studied by mixing increasing concentrations of reduced *Mt*AhpE (0.5 - 2.5 μM) and TNB (74 μM) in one syringe with H_2O_2 (20 μM) in the other syringe, at pH 7.4 and 25ºC, and recording TNB absorbance at 412 nm. The rate constant of reduced *Mt*AhpE oxidation by DTNB was determined by measuring initial rates of TNB formation from the reaction between reduced *Mt*AhpE (6 μM) with DTNB (100-500 μM) at pH 7.4 and 25ºC.

Results

*Mt*AhpE oxidation and overoxidation are accompanied by significant structural changes

Changes on MtAhpE fluorescence intensity. When recombinant His-tagged *Mt*AhpE (1.5 μM) was exposed to H_2O_2 (0.85 μM), an important decrease in the intrinsic fluorescence intensity was observed (Fig.1A). This change was reverted by reduction with DTT (1 mM), wich recovered intensities to even higher levels than initially (Fig. 1A). This is in agreement with the fact that the enzyme used had been stored for some days and was only partially reduced. No change in the fluorescence intensity was observed when either reduced *Mt*AhpE previously treated with NEM or *Mt*AhpEC45S were exposed to the same treatments (not shown). These data confirm that the oxidation of the peroxidatic (and single) cysteine of *Mt*AhpE is required for the observed fluorescence intensity changes. Moreover, when pre-reduced *Mt*AhpE (1 μM) was treated with a large excess of H_2O_2 (300 μM), there was an initial fast decrease followed by a slower increase in protein fluorescence intensity (Fig. 1B). Again, these changes were precluded by pretreatment of the enzyme with NEM in excess (not shown), indicating the participation of the cysteine residue in the process, and supporting that H_2O_2-dependent overoxidation of the sulfenic acid of the oxidized enzyme (C_P-SOH) to sulfinic acid (C_P-SO_2H) was responsible for the fluorescence recovery (see below).

MtAhpE quaternary structure is dependent on its oxidation state. Reduced *Mt*AhpE migrated as a monomer and only a slight fraction of oxidized enzyme formed intramolecular disulfides when analyzed by non-reducing SDS-PAGE electrophoresis (not shown). Reduced enzyme (60 μM) eluted as a unique peak with an elution volume

corresponding to a dimer (Fig. 2A, solid line). Oxidation of the enzyme with an equimolar amount of H_2O_2 resulted in the slow formation of higher molecular weight species, while addition of excess H_2O_2 to promote enzyme overoxidation resulted again in a dimeric form (Fig. 2A). The higher molecular weight species formed after incubation with equimolar H_2O_2 were reversed by the addition of 1 mM DTT (Fig. 2B). Interestingly, addition of 1 mM N-acetylcysteine (NAC, low molecular weight thiol that can be formed from mycothiol enzymatic degradation in *M. tuberculosis* (*53*)) to *Mt*AhpE treated with equimolar H_2O_2, resulted in a destabilization of the dimer, leading to lower molecular weight species (Fig. 2B). This could be due to the formation of a mixed disulfide through the reaction between the cysteine sulfenic acid (C_P-SOH) in oxidized *Mt*AhpE and the thiol group of NAC, as confirmed by mass spectrometry (see below). These results show that the quaternary structure of the protein is tightly controlled by the redox state of the peroxidatic cysteine.

Mass spectrometry analysis of cysteine modifications in *Mt*AhpE

Recently purified enzyme without further additions displayed a molecular mass of 19319 Da (Fig. 3A).When *Mt*AhpE (50 µM) was incubated with excess NEM (5 mM during 30 min), the observed shift in molecular weight was consistent with the complete alkylation of C_P, indicating a $k > 0.5\ M^{-1}s^{-1}$ for the reaction at pH 7.4 and 25ºC (Fig. 3B). Upon oxidation of *Mt*AhpE (50 µM) with equimolar H_2O_2 we were unable to detect the free sulfenic acid form of the enzyme. In the search for potential traps for sulfenic acid in oxidized *Mt*AhpE, the enzyme was exposed to equimolar H_2O_2 and two minutes latter, it was incubated with excess DTT, NAC or GSH. In the first case, a peak of 19319 Da was observed (Fig. 3C), corresponding to the reduced enzyme. Incubation with NAC or GSH caused a mass shift of + 162 and + 306, respectively (Fig. 3D and

3E), due to the formation of mixed disulfides with the oxidized enzyme. Finally, upon exposure of the enzyme (50 μM) to excess H_2O_2 (250 μM) for 2 min, a mass increment of 32 Da was detected, consistent with the addition of two oxygen atoms (Fig. 3F).

Kinetics of enzyme oxidation by peroxynitrite

Direct approach determinations. Addition of increasing concentrations of excess peroxynitrite led to a dose-dependent increase in the observed rate constants of *Mt*AhpE intrinsic fluorescence change (Fig. 4A, line a and inset). Changes were not observed when C45S mutated enzyme was used (Fig. 4A, line b), or by mixing wild type enzyme with peroxynitrite decomposition products (Fig. 4A, line c). From the slope of the plot shown in Fig. 4A inset, a second order rate constant of $(1.9 \pm 0.2) \times 10^7$ $M^{-1}s^{-1}$ at pH 7.4 and 25 ºC was determined.

Competition approach measurements. The reaction between reduced *Mt*AhpE and peroxynitrite was also studied by competition with HRP. As expected, increasing concentrations of *Mt*AhpE inhibited peroxynitrite-mediated HRP-compound I formation (Fig. 4B, inset). From these data the second order rate constant for peroxynitrite reduction by *Mt*AhpE was calculated as $(1.7 \pm 0.6) \times 10^7$ $M^{-1}s^{-1}$ at pH 7.4 and 25 ºC, in close agreement with the value obtained by the fluorescence approach. Total compound I formation at different *Mt*AhpE concentrations were consistent with yields expected according to computer-assisted simulations, assuming a simple competition system (Fig. 4B).

Kinetics of enzyme oxidation by H_2O_2

Direct approach determinations. Mixing with increasing concentrations of excess H_2O_2 led to a dose-dependent increase in the observed rate constants of *Mt*AhpE

fluorescence intensity change (Fig. 5A). The second order rate constant of this reaction was determined as (8.2 ± 1.5) x 10^4 $M^{-1}s^{-1}$ at pH 7.4 and 25ºC (Fig. 5A, inset).

Second order rate constants for H_2O_2-mediated *Mt*AhpE oxidation were faster at alkaline pHs (Fig 5B), indicating that thiolate in C_P was the reacting species, in agreement with previously proposed mechanism of reaction (*54, 55*). *Mt*AhpE was unstable and precipitated under low pH conditions (data not shown), thus limiting the pH range of our studies (pHs > 4.5), Amplitudes of fluorescence change decreased at acidic pH, but still k_{obs} values linearly depended on oxidant concentration. The pK_a of the peroxidatic thiol was estimated as 5.2. This is, to our knowledge, the first pK_a value reported for a 1-Cys Prx.

Competition approach measurements. In order to confirm the value for k_2 for H_2O_2-mediated *Mt*AhpE oxidation obtained above, the reaction was also studied by a competition approach (*44, 45*). Up to 15 µM *Mt*AhpE failed to inhibit compound I formation from the reaction between HRP (1 µM) and 0.75 µM H_2O_2 (not shown). Since the reaction of H_2O_2 with HRP is two orders of magnitude faster than with *Mt*AhpE according to the direct approach, high quantities of *Mt*AhpE (>100 fold excess over HRP) would be required to inhibit HRP-compound I formation. So, we selected another peroxidase, lignine peroxidase (LiP) (E.C. 1.11.1.14) which is known to react with H_2O_2 to form compound I with a slower rate constant than HRP. The addition of increasing concentrations of reduced *Mt*AhpE produced a dose-dependent inhibition of LiP–compound I formation (Fig. 5C). The second-order rate constant for H_2O_2 reduction by *Mt*AhpE was calculated as (7 ± 3) x 10^4 $M^{-1}s^{-1}$ at pH 7.4 and 25ºC, which is in excellent agreement with the value obtained by the fluorimetric approach.

Kinetics of enzyme overoxidation by H_2O_2

The kinetics of H_2O_2-mediated *Mt*AhpE overoxidation to sulfinic acid was studied by taking advantage of the increase in intrinsic fluorescence intensity that took place during oxidized *Mt*AhpE exposure to high excess oxidant concentrations, as observed in Fig. 1B. Addition of increasing concentrations of H_2O_2 (100-500 μM) caused a dose dependent increase in the observed rate constants of the intrinsic fluorescence change of *Mt*AhpE (1 μM), and a rate constant of 40 ± 3 $M^{-1}s^{-1}$ at pH 7.4 and 25ºC was determined. The enzyme previously incubated with NEM (5 mM, 30 minutes) exhibited no significant change in its fluorescence intensity (Fig. 6A), that together with the +32 increase in protein molecular weight (Fig. 3F), confirmed that the mentioned change was due to C_P overoxidation.

Apparent second order rate constant of overoxidation were higher al alkaline pHs (Fig. 6B), indicating a mechanism of reaction where sulfenate reacted with H_2O_2. The pH independent rate constant of the reaction was 42 ± 2 $M^{-1}s^{-1}$. A pK_a value for *Mt*AhpE sulfenic acid of 6.6 ± 0.1 was determined, very similar to the pK_a value previously reported for the sulfenic acid intermediate formed in *Salmonella typhimurium* AhpC, a typical two-cysteine Prx (*56*).

Catalytic consumption of hydrogen peroxide with thionitrobenzoate as reductant

When reduced *Mt*AhpE (2.5 μM) and TNB (70 μM) were mixed with H_2O_2 (20 μM), a decrease in TNB concentration was observed (Fig. 7A). Under our experimental conditions, and considering the second-order rate constant reported herein, H_2O_2-mediated *Mt*AhpE oxidation to sulfenic acid occurs almost immediately ($t_{1/2}$ = 0. 42 s). Furthermore, the oxidation of TNB by H_2O_2 is negligible (k = 0.45 $M^{-1}s^{-1}$ at pH 7.4 and

25ºC, data not shown). Thus, any decrease in TNB concentration observed would be due to its reaction with oxidized enzyme. Time courses of the reaction were biphasic, with a rapid phase that lasted about 15 s followed by a slower TNB oxidation. Data fitted an exponential plus straight line equation,

$$[\text{TNB}] = A \exp(- k_{obs} t) + S t + \text{offset} \quad (4)$$

where A represents the amplitude, k_{obs} is the pseudo-first-order rate constant of the first phase and S represents the slope of the second phase. The biphasic decay in TNB thus presented typical pre steady-state kinetics, where the fast consumption of TNB by sulfenic acid (burst) was followed by the rate limiting turnover of the enzyme. Thus, in addition to reactivity to sulfenic acid to form a mixed disulfide, TNB reacted with the latter yielding the reduced form of the enzyme which in turn could be again oxidized by H_2O_2 constituting a catalytic cycle:

$$\textit{Mt}\text{AhpE-SH} + H_2O_2 \rightarrow \textit{Mt}\text{AhpE-SOH} + OH^- \quad \text{(very fast)} \quad (5)$$

$$\textit{Mt}\text{AhpE-SOH} + \text{TNB} \rightarrow \textit{Mt}\text{AhpE-STNB} + OH^- \quad \text{(fast)} \quad (6)$$

$$\textit{Mt}\text{AhpE-STNB} + \text{TNB} \rightleftharpoons \textit{Mt}\text{AhpE-SH} + \text{DTNB} \quad \text{(slow)} \quad (7)$$

The reaction finished after ~60 min and the total consumption of TNB was twice the concentration of H_2O_2 used, confirming the catalytic mechanism proposed (not shown). The amplitude of the exponential phase was proportional to the enzyme concentration as expected for burst kinetics (Fig. 7A, inset) and represented the amount of sulfenic acid that could be detected through mixed disulfide formation in our conditions, 77 % of *Mt*AhpE. The rate constant for the reaction of TNB with sulfenic acid (Eq. 6), was

calculated after dividing k_{obs} by [TNB] as 1.5 ± 0.3 x 10^3 $M^{-1}s^{-1}$ and was independent of the enzyme concentration (data not shown). The rate constant for the reaction between the mixed disulfide and TNB (Eq. 7) was estimated from the plot of –(S) *versus* A (i.e. *Mt*AhpE-STNB concentration), after dividing the slope by TNB concentration, giving a value of 266 M^{-1} s^{-1} (Fig. 7B). Finally, the rate constant of the reaction between reduced *Mt*AhpE and DTNB (reverse of Eq. 7) was measured as 180 ± 9 M^{-1} s^{-1} at pH 7.4 and 25 °C (not shown).

Discussion

Oxidation of recombinant *Mt*AhpE occurred with a rapid decrease in its fluorescence intensity, which was reverted by DTT (Fig. 1A), as well as by the addition of high excess concentrations of the oxidant (Fig. 1B). These changes occurred when exciting either at 280 (not shown) or 295 nm (Figs. 1 A and 1B), indicating that at least one of the three tryptophan residues present in the protein sequence is involved in the process. Changes in fluorescence intensity pointed towards structural modifications of the protein under different redox states, which caused differential quenching of tryptophan fluorescence by neighboring, not yet identified, amino acid residues (*57*). Reduced *Mt*AhpE was a non-covalent dimer in solution, and oligomerized upon treatment with equimolar concentrations of H_2O_2. These changes in quaternary structure were much slower, and thus were not responsible, for the fluorescence intensity decrease (Fig. 2A), and were reverted by protein reduction (Fig. 2B). Oligomerization did not occur when the enzyme was exposed to high excess oxidant concentrations that caused overoxidation (Fig. 2A). These data are consistent with the reported crystallography structure of *Mt*AhpE, that evidenced important differences in conformation at reduced *versus* oxidized states[4] (*24*). Although the structure of the overoxidized form of the enzyme is not available, our data suggests that reduced and overoxidized forms of *Mt*AhpE have similar conformations, as reported for 2-Cys Prxs (*36*). Oxidation of the thiol by equimolar peroxide concentrations led to sulfenic acid formation, that was trapped by GSH, NAC and TNB leading to mixed disulfides formation (Figs. 3D, 3E and 7A), and that was reduced by DTT and TNB (Figs. 3C and 7B). This is in agreement with crystallography data that showed that that the cysteine

[4]Although the crystal structure of reduced enzyme reported was composed by two asymmetric dimers (*24*), for which we found no evidence in our gel filtration experiments, probably reflecting different experimental conditions and /or labile enzyme dimer association.

residue was oxidized to sulfenic acid in the oxidized form of the enzyme (*24*), and with our results indicating that only a slight fraction of the enzyme formed intermolecular disulfides upon oxidation.

The fact that observed rate constant of fluorescence decrease showed a linear relationship with oxidant concentration indicated that oxidation was rate-limiting the overall process leading to changes in fluorescent intensity (Fig. 4A and 5A). This was confirmed by using alternative approaches based on competition kinetics that yielded very similar *k* values (Fig 4A *versus* Fig. 4B; Fig. 5A *versus* Fig 5C). As in the case of human Prx5, but contrary to what we observed for human red blood cell Prx2, or was reported for mammal Prx 6, bacterial AhpC or yeast TSA1 and TSA2, peroxynitrite-mediated *Mt*AhpE oxidation was at least two orders of magnitude faster than that mediated by H_2O_2 (Table I), indicating that the enzyme is a highly selective peroxidase. In general, kinetics of reactions of low molecular weight thiols with different peroxides follow the trend indicated by Edwards, *i.e.* those peroxides with the lower pK_a of the leaving group react faster than the others (*58*). The trend appears to be maintained in the case of *Mt*AhpE C_P, at least for the peroxides tested so far. However, it is lost in many Prxs (*46*). Thus, the molecular basis for oxidizing substrate specificity in Prxs is intriguing, and its rationalization will require a thorough combined analysis of kinetic and structural data for Prxs of different subfamilies.

Thiolates are known to be the nucleophile species during peroxide reduction, and therefore peroxidatic thiol pK_a could affect this reactivity. In the case of *Mt*AhpE this was 5.2 (Fig. 4b), being the first determination for a 1-Cys Prx. A low pK_a value indicates that the thiol would be almost totally in its reactive form at pHs the enzyme is expected to encounter *in vivo*. This value is similar to those reported for other, 2-cys Prxs (<5-6.3, (*59*)), in agreement with the similar active site geometry.

*Mt*AhpE catalytic activity requires sulfenic acid reduction. Oxidized *Mt*AhpE formed mixed disulfides with different monothiols tested (Figs 3 D and E). For selected 1-Cys Prxs, mixed disulfide formation with GSH and their reduction have been reported (*29, 30, 32*). However, *Mycobacteria* lack glutathione and contain a particular sets of low molecular weight thiols (*10*) and thiol-disulfide reductases (*13*), and evidences for enzymatic routes for *Mt*AhpE-mixed disulfide reduction, is lacking so far. Although we did not identify potential natural reducing substrates for the enzyme, we succeeded in designing a spectrophotometric method for easily measuring catalytic activity using the artificial reductant TNB. This reagent also allowed detecting and quantifying sulfenic acid in oxidized *Mt*AhpE (Fig. 7).

As above mentioned, excess H_2O_2 led to a rapid decreased followed by a slower increase in *Mt*AhpE fluorescence intensity that were precluded by thiol alkylation (Fig. 1b and Fig 5a). The observed rate constant of the second phase was linearly dependent on H_2O_2 concentration again indicating that the bimolecular reaction was the rate-limiting step of the process (Fig 6A), and a +32 molecular weight increase was detected (Fig. 3F). Altogether, these data are indicative of H_2O_2-mediated thiol overoxidation to sulfinic acid with a rate constant of 40 ± 3 $M^{-1}s^{-1}$ at pH 7.4 and 25ºC. This value is very similar to the 57 $M^{-1}s^{-1}$ calculated previously for Prx 1 inactivation (*35, 36*), and much faster than reported rate constants for H_2O_2- mediated oxidation of sulfenic acid in human serum albumin or streptococcal NADH peroxidase ($k = 0.4 \pm 0.2$ $M^{-1}s^{-1}$ and 0.14 $M^{-1}s^{-1}$, respectively (*39, 60*)). Moreover, rate constants of H_2O_2-mediated sulfenic acid oxidation were faster at alkaline pH, consistent with a mechanism of reaction where sulfenate is the reactive species, suggesting nucleophilic attack on the peroxidic oxygen (followed by rearrangement to sulfinic acid). The pH profile for this reaction allowed us to calculate the pK_a of the sulfenic acid at the oxidized enzyme as 6.6 ± 0.1 (Fig. 5B),

very similar to the reported pK_a (= 6.1) of the sulfenic acid intermediate formed during peroxidatic thiol oxidation in the bacterial 2-Cys Prx AhpC (*56*). Since intrabacterial pH of wild type *M. tuberculosis* inside both non-activated and IFN-γ-activated macrophages has been reported as 6.8–7.5 (*61*), > 95 % thiol and > 50 % sulfenic acid would be deprotonated and therefore, at their reactive form with peroxides, in reduced and oxidized *Mt*AhpE, respectively. Oxidative inactivation susceptibility is dictated by the competition between two processes: sulfenic acid oxidation to sulfinic acid *vs* its resolution. Our data gives experimental support to the idea originally proposed by Wood et al (*36*), indicating that rates of sulfenic acid oxidation are similar for different Prxs, and that susceptibility to inactivation by overoxidation depends mainly in different rates of sulfenic acid reaction with the resolving thiol or substrate(s).

In conclusion, this work contributes to the functional characterization of the one-cysteine Prx codified in the genome of *M. tuberculosis*, *Mt*AhpE, for which evidence of expression already exists at a transcriptional level (*23*). Its rapid reaction with peroxynitrite, which resulted as fast as with *Mt*TPx and ten fold faster than with catalase peroxidase (*9, 15, 62*), suggests that *Mt*AhpE represents an important antioxidant defense against this cytotoxic molecule, which can be formed by activated macrophages during infection (*63*). On the contrary, other *M. tuberculosis* enzymes, especially *Mt*AhpC and catalase peroxidase, reduced H_2O_2 with a greater rate constant than *Mt*AhpE (*64, 65*). However, it is important to consider at this point that preferential routes for peroxide reduction would be dictated not only by the rate constant, *k*, but by rates of reaction (*k* x [target]). Concentrations of these enzymes are mostly unknown in *M. tuberculosis* and may change depending on different conditions (*66*). Thus, our *in vitro* data provide kinetic evidences indicating that *Mt*AhpE could play a role for selected cytotoxic peroxide detoxification, especially peroxynitrite, but further

investigation will be required to understand its role in *M. tuberculosis* pathobiology. In this regard, it should be noted that although peroxidatic active site structure is conserved among different Prxs, *Mt*AhpE structure differs in some aspects from Prxs present in mammal cells (*24*). Therefore, its functional and structural characterization is not only an important step towards the understanding the bacterial mechanisms of antioxidant defense, but could also facilitate future investigation regarding its validation as a potential drug target for the treatment of the tuberculosis disease.

Aknowledgements

We thank Dr. Pedro Alzari from Institut Pasteur Paris, France, for kindly provinding the plasmid of His-tag *Mt*AhpE and Dr. Gonzalo Peluffo from Universidad de la República, Uruguay, for assistance in mass spectrometry determinations.

References

1. WHO Report. (2009) Global Tuberculosis Control EPIDEMIOLOGY, STRATEGY, FINANCING, pp 6-33, World Health Organization.
2. Zahrt, T. C., and Deretic, V. (2002) Reactive nitrogen and oxygen intermediates and bacterial defenses: unusual adaptations in Mycobacterium tuberculosis, *Antioxid Redox Signal 4*, 141-159.
3. Fang, F. C. (2004) Antimicrobial reactive oxygen and nitrogen species: concepts and controversies, *Nat Rev Microbiol 2*, 820-832.
4. Nathan, C., and Shiloh, M. U. (2000) Reactive oxygen and nitrogen intermediates in the relationship between mammalian hosts and microbial pathogens, *Proc Natl Acad Sci U S A 97*, 8841-8848.
5. Shiloh, M. U., and Nathan, C. F. (2000) Reactive nitrogen intermediates and the pathogenesis of Salmonella and mycobacteria, *Curr Opin Microbiol 3*, 35-42.
6. MacMicking, J. D., North, R. J., LaCourse, R., Mudgett, J. S., Shah, S. K., and Nathan, C. F. (1997) Identification of nitric oxide synthase as a protective locus against tuberculosis, *Proc Natl Acad Sci U S A 94*, 5243-5248.
7. Nozaki, Y., Hasegawa, Y., Ichiyama, S., Nakashima, I., and Shimokata, K. (1997) Mechanism of nitric oxide-dependent killing of Mycobacterium bovis BCG in human alveolar macrophages, *Infect Immun 65*, 3644-3647.
8. Manca, C., Paul, S., Barry, C. E., 3rd, Freedman, V. H., and Kaplan, G. (1999) Mycobacterium tuberculosis catalase and peroxidase activities and resistance to oxidative killing in human monocytes in vitro, *Infect Immun 67*, 74-79.

9. Jaeger, T., Budde, H., Flohe, L., Menge, U., Singh, M., Trujillo, M., and Radi, R. (2004) Multiple thioredoxin-mediated routes to detoxify hydroperoxides in Mycobacterium tuberculosis, *Arch Biochem Biophys 423*, 182-191.

10. Newton, G. L., Arnold, K., Price, M. S., Sherrill, C., Delcardayre, S. B., Aharonowitz, Y., Cohen, G., Davies, J., Fahey, R. C., and Davis, C. (1996) Distribution of thiols in microorganisms: mycothiol is a major thiol in most actinomycetes, *J Bacteriol 178*, 1990-1995.

11. Patel, M. P., and Blanchard, J. S. (1999) Expression, purification, and characterization of Mycobacterium tuberculosis mycothione reductase, *Biochemistry 38*, 11827-11833.

12. Ordonez, E., Van Belle, K., Roos, G., De Galan, S., Letek, M., Gil, J. A., Wyns, L., Mateos, L. M., and Messens, J. (2009) Arsenate reductase, mycothiol, and mycoredoxin concert thiol/disulfide exchange, *J Biol Chem 284*, 15107-15116.

13. den Hengst, C. D., and Buttner, M. J. (2008) Redox control in actinobacteria, *Biochim Biophys Acta 1780*, 1201-1216.

14. Timmins, G. S., and Deretic, V. (2006) Mechanisms of action of isoniazid, *Mol Microbiol 62*, 1220-1227.

15. Wengenack, N. L., Jensen, M. P., Rusnak, F., and Stern, M. K. (1999) Mycobacterium tuberculosis KatG is a peroxynitritase, *Biochem Biophys Res Commun 256*, 485-487.

16. Wengenack, N. L., and Rusnak, F. (2001) Evidence for isoniazid-dependent free radical generation catalyzed by Mycobacterium tuberculosis KatG and the isoniazid-resistant mutant KatG(S315T), *Biochemistry 40*, 8990-8996.

17. Sherman, D. R., Mdluli, K., Hickey, M. J., Arain, T. M., Morris, S. L., Barry, C. E., 3rd, and Stover, C. K. (1996) Compensatory ahpC gene expression in isoniazid-resistant Mycobacterium tuberculosis, *Science 272*, 1641-1643.

18. Hu, Y., and Coates, A. R. (2009) Acute and persistent Mycobacterium tuberculosis infections depend on the thiol peroxidase TpX, *PLoS ONE 4*, e5150.

19. Cole, S. T., Brosch, R., Parkhill, J., Garnier, T., Churcher, C., Harris, D., Gordon, S. V., Eiglmeier, K., Gas, S., Barry, C. E., 3rd, Tekaia, F., Badcock, K., Basham, D., Brown, D., Chillingworth, T., Connor, R., Davies, R., Devlin, K., Feltwell, T., Gentles, S., Hamlin, N., Holroyd, S., Hornsby, T., Jagels, K., Krogh, A., McLean, J., Moule, S., Murphy, L., Oliver, K., Osborne, J., Quail, M. A., Rajandream, M. A., Rogers, J., Rutter, S., Seeger, K., Skelton, J., Squares, R., Squares, S., Sulston, J. E., Taylor, K., Whitehead, S., and Barrell, B. G. (1998) Deciphering the biology of Mycobacterium tuberculosis from the complete genome sequence, *Nature 393*, 537-544.

20. Kang, G. Y., Park, E. H., Kim, K., and Lim, C. J. (2009) Overexpression of bacterioferritin comigratory protein (Bcp) enhances viability and reduced glutathione level in the fission yeast under stress, *J Microbiol 47*, 60-67.

21. Limauro, D., Pedone, E., Galdi, I., and Bartolucci, S. (2008) Peroxiredoxins as cellular guardians in Sulfolobus solfataricus: characterization of Bcp1, Bcp3 and Bcp4, *Febs J 275*, 2067-2077.

22. Passardi, F., Theiler, G., Zamocky, M., Cosio, C., Rouhier, N., Teixera, F., Margis-Pinheiro, M., Ioannidis, V., Penel, C., Falquet, L., and Dunand, C. (2007) PeroxiBase: the peroxidase database, *Phytochemistry 68*, 1605-1611.

23. Murphy, D. J., and Brown, J. R. (2007) Identification of gene targets against dormant phase Mycobacterium tuberculosis infections, *BMC Infect Dis 7*, 84.

24. Li, S., Peterson, N. A., Kim, M. Y., Kim, C. Y., Hung, L. W., Yu, M., Lekin, T., Segelke, B. W., Lott, J. S., and Baker, E. N. (2005) Crystal Structure of AhpE from Mycobacterium tuberculosis, a 1-Cys peroxiredoxin, *J Mol Biol 346*, 1035-1046.

25. Wood, Z. A., Poole, L. B., Hantgan, R. R., and Karplus, P. A. (2002) Dimers to doughnuts: redox-sensitive oligomerization of 2-cysteine peroxiredoxins, *Biochemistry 41*, 5493-5504.

26. Poole, L. B. (2007) The catalytic mechanism of peroxiredoxins, *Subcell Biochem 44*, 61-81.

27. Choi, H. J., Kang, S. W., Yang, C. H., Rhee, S. G., and Ryu, S. E. (1998) Crystal structure of a novel human peroxidase enzyme at 2.0 A resolution, *Nat Struct Biol 5*, 400-406.

28. Rhee, S. G., Chae, H. Z., and Kim, K. (2005) Peroxiredoxins: a historical overview and speculative preview of novel mechanisms and emerging concepts in cell signaling, *Free Radic Biol Med 38*, 1543-1552.

29. Ralat, L. A., Manevich, Y., Fisher, A. B., and Colman, R. F. (2006) Direct evidence for the formation of a complex between 1-cysteine peroxiredoxin and glutathione S-transferase pi with activity changes in both enzymes, *Biochemistry 45*, 360-372.

30. Ralat, L. A., Misquitta, S. A., Manevich, Y., Fisher, A. B., and Colman, R. F. (2008) Characterization of the complex of glutathione S-transferase pi and 1-cysteine peroxiredoxin, *Arch Biochem Biophys 474*, 109-118.

31. Monteiro, G., Horta, B. B., Pimenta, D. C., Augusto, O., and Netto, L. E. (2007) Reduction of 1-Cys peroxiredoxins by ascorbate changes the thiol-specific antioxidant paradigm, revealing another function of vitamin C, *Proc Natl Acad Sci U S A 104*, 4886-4891.

32. Greetham, D., and Grant, C. M. (2009) Antioxidant activity of the yeast mitochondrial one-Cys peroxiredoxin is dependent on thioredoxin reductase and glutathione in vivo, *Mol Cell Biol 29*, 3229-3240.

33. Pedrajas, J. R., Miranda-Vizuete, A., Javanmardy, N., Gustafsson, J. A., and Spyrou, G. (2000) Mitochondria of Saccharomyces cerevisiae contain one-conserved cysteine type peroxiredoxin with thioredoxin peroxidase activity, *J Biol Chem 275*, 16296-16301.

34. Kim, S. Y., Jo, H. Y., Kim, M. H., Cha, Y. Y., Choi, S. W., Shim, J. H., Kim, T. J., and Lee, K. Y. (2008) H2O2-dependent hyperoxidation of peroxiredoxin 6 (Prdx6) plays a role in cellular toxicity via up-regulation of iPLA2 activity, *J Biol Chem 283*, 33563-33568.

35. Stone, J. R. (2004) An assessment of proposed mechanisms for sensing hydrogen peroxide in mammalian systems, *Arch Biochem Biophys 422*, 119-124.

36. Wood, Z. A., Poole, L. B., and Karplus, P. A. (2003) Peroxiredoxin evolution and the regulation of hydrogen peroxide signaling, *Science 300*, 650-653.

37. Beckman, J. S., Beckman, T. W., Chen, J., Marshall, P. A., and Freeman, B. A. (1990) Apparent hydroxyl radical production by peroxynitrite: implications for endothelial injury from nitric oxide and superoxide, *Proc Natl Acad Sci U S A 87*, 1620-1624.

38. Radi, R., Beckman, J. S., Bush, K. M., and Freeman, B. A. (1991) Peroxynitrite oxidation of sulfhydryls. The cytotoxic potential of superoxide and nitric oxide, *J Biol Chem 266*, 4244-4250.

39. Turell, L., Botti, H., Carballal, S., Ferrer-Sueta, G., Souza, J. M., Duran, R., Freeman, B. A., Radi, R., and Alvarez, B. (2008) Reactivity of sulfenic acid in human serum albumin, *Biochemistry 47*, 358-367.

40. Claiborne, A., Miller, H., Parsonage, D., and Ross, R. P. (1993) Protein-sulfenic acid stabilization and function in enzyme catalysis and gene regulation, *Faseb J 7*, 1483-1490.

41. Pace, C. N., Vajdos, F., Fee, L., Grimsley, G., and Gray, T. (1995) How to measure and predict the molar absorption coefficient of a protein, *Protein Sci 4*, 2411-2423.

42. Schonbaum, G. R., and Lo, S. (1972) Interaction of peroxidases with aromatic peracids and alkyl peroxides. Product analysis, *J Biol Chem 247*, 3353-3360.

43. Tien, M., Kirk, T. K., Bull, C., and Fee, J. A. (1986) Steady-state and transient-state kinetic studies on the oxidation of 3,4-dimethoxybenzyl alcohol catalyzed by the ligninase of Phanerocheate chrysosporium Burds, *J Biol Chem 261*, 1687-1693.

44. Ogusucu, R., Rettori, D., Munhoz, D. C., Netto, L. E., and Augusto, O. (2007) Reactions of yeast thioredoxin peroxidases I and II with hydrogen peroxide and peroxynitrite: rate constants by competitive kinetics, *Free Radic Biol Med 42*, 326-334.

45. Peskin, A. V., Low, F. M., Paton, L. N., Maghzal, G. J., Hampton, M. B., and Winterbourn, C. C. (2007) The high reactivity of peroxiredoxin 2 with H(2)O(2)

is not reflected in its reaction with other oxidants and thiol reagents, *J Biol Chem 282*, 11885-11892.

46. Trujillo, M., Clippe, A., Manta, B., Ferrer-Sueta, G., Smeets, A., Declercq, J. P., Knoops, B., and Radi, R. (2007) Pre-steady state kinetic characterization of human peroxiredoxin 5: taking advantage of Trp84 fluorescence increase upon oxidation, *Arch Biochem Biophys 467*, 95-106.

47. Manta, B., Hugo, M., Ortiz, C., Ferrer-Sueta, G., Trujillo, M., and Denicola, A. (2008) The peroxidase and peroxynitrite reductase activity of human erythrocyte peroxiredoxin 2, *Arch Biochem Biophys 484,* 146-154.

48. Hayashi, Y., and Yamazaki, I. (1979) The oxidation-reduction potentials of compound I/compound II and compound II/ferric couples of horseradish peroxidases A2 and C, *J Biol Chem 254*, 9101-9106.

49. Floris, R., Piersma, S. R., Yang, G., Jones, P., and Wever, R. (1993) Interaction of myeloperoxidase with peroxynitrite. A comparison with lactoperoxidase, horseradish peroxidase and catalase, *Eur J Biochem 215*, 767-775.

50. Mendes, P. (1993) GEPASI: a software package for modelling the dynamics, steady states and control of biochemical and other systems, *Comput. Appl. Biosci. 9*, 563-571.

51. Mendes, P. (1997) Biochemistry by numbers: simulation of biochemical pathways with Gepasi 3., *Trends Biochem. Sci. 22*, 361-363.

52. Peshenko, I. V., and Shichi, H. (2001) Oxidation of active center cysteine of bovine 1-Cys peroxiredoxin to the cysteine sulfenic acid form by peroxide and peroxynitrite, *Free Radic Biol Med 31*, 292-303.

53. Steffek, M., Newton, G. L., Av-Gay, Y., and Fahey, R. C. (2003) Characterization of Mycobacterium tuberculosis mycothiol S-conjugate amidase, *Biochemistry 42*, 12067-12076.

54. Hofmann, B., Hecht, H. J., and Flohe, L. (2002) Peroxiredoxins, *Biol Chem 383*, 347-364.

55. Wood, Z. A., Schroder, E., Harris, R. J., and Poole, L. B. (2003) Structure, mechanism and regulation of peroxiredoxins, *Trends Biochem Sci 28*, 32-40.

56. Poole, L. B., and Ellis, H. R. (2002) Identification of cysteine sulfenic acid in AhpC of alkyl hydroperoxide reductase, *Methods Enzymol 348*, 122-136.

57. Lakowicz, J. R. (1999) *Principles of Fluorescence Spectroscopy, 2nd ed.*, New York.

58. Edwards, J. O. (1962) Nucleophilic displacement on oxygen in peroxides., in *Peroxide Reaction Mechanisms* (Edwards, J. O., Ed.), pp 67–106, Interscience, New York.

59. Trujillo, M., Ferrer-Sueta, G., and Radi, R. (2008) Peroxynitrite detoxification and its biologic implications, *Antioxid Redox Signal 10*, 1607-1620.

60. Poole, L. B., and Claiborne, A. (1989) The non-flavin redox center of the streptococcal NADH peroxidase. II. Evidence for a stabilized cysteine-sulfenic acid, *J Biol Chem 264*, 12330-12338.

61. Vandal, O. H., Pierini, L. M., Schnappinger, D., Nathan, C. F., and Ehrt, S. (2008) A membrane protein preserves intrabacterial pH in intraphagosomal Mycobacterium tuberculosis, *Nat Med 14*, 849-854.

62. Bryk, R., Griffin, P., and Nathan, C. (2000) Peroxynitrite reductase activity of bacterial peroxiredoxins, *Nature 407*, 211-215.

63. Alvarez, M. N., Piacenza, L., Irigoin, F., Peluffo, G., and Radi, R. (2004) Macrophage-derived peroxynitrite diffusion and toxicity to Trypanosoma cruzi, *Arch Biochem Biophys 432*, 222-232.

64. Jakopitsch, C., Vlasits, J., Wiseman, B., Loewen, P. C., and Obinger, C. (2007) Redox intermediates in the catalase cycle of catalase-peroxidases from Synechocystis PCC 6803, Burkholderia pseudomallei, and Mycobacterium tuberculosis, *Biochemistry 46*, 1183-1193.

65. Parsonage, D., Karplus, P. A., and Poole, L. B. (2008) Substrate specificity and redox potential of AhpC, a bacterial peroxiredoxin, *Proc Natl Acad Sci U S A 105*, 8209-8214.

66. Springer, B., Master, S., Sander, P., Zahrt, T., McFalone, M., Song, J., Papavinasasundaram, K. G., Colston, M. J., Boettger, E., and Deretic, V. (2001) Silencing of oxidative stress response in Mycobacterium tuberculosis: expression patterns of ahpC in virulent and avirulent strains and effect of ahpC inactivation, *Infect Immun 69*, 5967-5973.

67. Dubuisson, M., Vander Stricht, D., Clippe, A., Etienne, F., Nauser, T., Kissner, R., Koppenol, W. H., Rees, J. F., and Knoops, B. (2004) Human peroxiredoxin 5 is a peroxynitrite reductase, *FEBS Lett 571*, 161-165.

68. Ogusucu, R., Rettori, D., Munhoz, D. C., Netto, L. E., and Augusto, O. (2007) Reactions of yeast thioredoxin peroxidases I and II with hydrogen peroxide and peroxynitrite: rate constants by competitive kinetics, *Free Radic Biol Med 42*, 326-334.

Table 1. Kinetics of H_2O_2 and peroxynitrite reduction by peroxiredoxins

Prx	Prx type	$k_{2\ H2O2}$ ($M^{-1}s^{-1}$)	$k_{2\ ONOOH}$ ($M^{-1}s^{-1}$)	Reference
S. typhimurium **AhpC**	typical 2-cys	[a]4 x 10^7		(*65*)
			[b]1.5 x 10^6	(*62*)
M. tuberculosis **AhpE**	1-cys	8.2 x 10^4	1.9 x 10^7	This work
M. tuberculosis **TPx**	atypical 2-cys	ND	1.5 x 10^7	(*9*)
H. sapiens **Prx 2**	typical 2-cys	1.3 x 10^7		(*45*)
		1.0 x 10^8	1.4 x 10^7	(*47*)
H. sapiens **Prx 5**	atypical 2-cys		7 x 10^7	(*67*)
		3 x 10^5	6.7 x 10^7	(*46*)
S. cerevisiae **Tsa1**	typical 2-cys	2.2 × 10^7	7.4 × 10^5	(*68*)
S. cerevisiae **Tsa2**	typical 2-cys	1.3 × 10^7	5.1 × 10^5	(*68*)

Rate constants were reported at pH 7.4 and 25°C unless otherwise indicated. ND is non-determined.

[a]at pH 7, [b]at pH 6.75, a similar value was reported for peroxynitrite reduction by *M. tuberculosis* AhpC (*62*)

Legends to figures

Figure 1. Intrinsic fluorescence of *Mt*AhpE under different redox states

A. Fluorescence emission spectra (λ_{ex} = 295 nm) of *Mt*AhpE (1.5 µM, 0.83 µM thiol) without any further addition (solid line), plus 0.85 µM H_2O_2 (dotted line) and plus 1 mM DTT (dashed line). **B.** Pre-reduced *Mt*AhpE (1.0 µM) without any further addition (solid line) or after addition of 300 µM H_2O_2 for 1 minute (dashed line) or 10 minutes (dotted line).

Figure 2. Redox-mediated changes in quaternary structure of *Mt*AhpE

A. Elution profiles of *Mt*AhpE on a Superdex 75 10/300 column. *Mt*AhpE (0.1 mg) was loaded onto a column previously equilibrated with 20 mM phosphate buffer, 150 mM NaCl, pH 7.4, with no previous treatment (solid line), upon incubation with equimolar H_2O_2 (1 min, dashed line; 60 min, dashed-dotted line) and after addition of 20 fold excess H_2O_2 (10 minutes, dotted line). Arrows indicate the position of molecular weight calibrants. From **a** to **d**: 67, 43, 25 and 13.7 KDa. **B.** Solid line, the same as in (**A**), after treatment with equimolar amounts of H_2O_2 for 60 minutes and with further addition of 1 mM DTT (dashed line) or 2 mM N-acetylcysteine (dotted line).

Figure 3. Covalent modifications of *Mt*AhpE cysteine residue

Electrospray ionization mass spectrometry analysis of *Mt*AhpE (50 µM) with no further treatment (**A**), incubated with 5 mM NEM during 30 minutes (**B**), oxidized with equimolar H_2O_2 for 1 min and then treated with either 1 mM DTT (**C**), 2 mM NAC (**D**) or 2mM GSH (**E**), and treated with excess H_2O_2 (250 µM) during 2 minutes (**F**).

Samples were desalted and diluted to 1 μM concentration for mass spectrometric analysis.

Figure 4. Kinetics of peroxynitrite-mediated *Mt*AhpE oxidation

A. Pre-reduced wild type (a) or C45S *Mt*AhpE (b) (0.25 μM) were rapidly mixed with peroxynitrite (1.15 and 3.3 μM, respectively) in sodium phosphate buffer 100 mM containing 0.1 mM dtpa, pH 7.4 and 25ºC, and the time-dependent decrease in total emission fluorescence intensity was determined. (c) As in (a) but using pre-decomposed peroxynitrite (3.3 μM). The gray trace represents the fit of experimental data in (a) to a single exponential function. *Inset*: effect of increasing peroxynitrite concentrations on the observed rate constants (k_{obs}) of fluorescence change. **B.** HRP (5 μM) was rapidly mixed with peroxynitrite (1.0 μM) in the presence of increasing concentrations of pre-reduced *Mt*AhpE. The concentration of compound I formed at each *Mt*AhpE concentration (squares) was determined. The continuous line represents the computer-assisted simulation of compound I yields according to a simple competition system using the calculated rate constant ($k_2 = 1.7 \pm 0.6 \times 10^7$ $M^{-1}s^{-1}$). *Inset*: time courses of HRP oxidation by peroxynitrite in the presence of increasing reduced *Mt*AhpE concentrations (from bottom to top 0, 0.47, 0.94, 1.9 and 2.8 μM).

Figure 5. Kinetics of H_2O_2-mediated *Mt*AhpE oxidation and peroxidatic thiol pK_a determination

A. Pre-reduced *Mt*AhpE (1.0 μM) was rapidly mixed with H_2O_2 (20 μM) in sodium phosphate buffer 100 mM containing 0.1 mM dtpa, pH 7.4 and 25ºC, and the time-dependent decrease in total emission fluorescence ($\lambda_{ex} = 280$ nm) was followed. The gray trace represents the best fit to a single exponential function. *Inset*: effect of

increasing H_2O_2 concentrations on the observed rate constants (k_{obs}) of fluorescence change, from which the apparent rate constant of the reaction at pH 7.4 was obtained.

B. Same as in (**A**), but performed in sodium acetate or sodium phosphate buffers of different pHs as indicated under Methods. Apparent second order rate constants for the reaction between reduced enzyme and H_2O_2 obtained (●) were plotted *vs* pH and data points were fitted to Eq. (3) (continuous line). **C.** Time courses of LiP (5 μM) oxidation by H_2O_2 (1.0 μM) in the presence of increasing concentrations of reduced *Mt*AhpE (from bottom to top 0, 3.3, 6.6, and 19.8 μM).

Figure 6. Kinetics of H_2O_2-mediated *Mt*AhpE overoxidation and sulfenic acid pK_a determination

A. Reduced (a) or alkylated (b) *Mt*AhpE (1.0 μM) were mixed with H_2O_2 (230 μM) in sodium phosphate buffer 100 mM containing 0.1 mM dtpa, pH 7.4 and 25ºC, and the time-dependent protein fluorescence increase (λ_{ex} = 295 nm, λ_{em} = 338 nm) was determined. The gray trace represents the fit of experimental data in (a) to a single exponential function. Inset: Effect of increasing H_2O_2 concentrations on the observed rate constants (k_{obs}) of fluorescence change, from which the apparent rate constant of the reaction at pH 7.4 was obtained. **B.** Same as in (**A**), but performed in sodium phosphate buffers 100 mM containing 0.1 mM dtpa of indicated pHs. Apparent second order rate constants for the reaction between reduced enzyme and H_2O_2 obtained (■) were plotted *vs* pH and data points were fitted to Eq. (3) (continuous line).

Figure 7. Catalytic reduction of *Mt*AhpE by TNB

A. Reduced *Mt*AhpE (2.5 μM) and TNB (70 μM) in one syringe were mixed with H_2O_2 (20 μM) in the second syringe using a stopped flow accessory. The decrease

in TNB concentration was followed at 412 nm (black trace). The gray trace represents the best fit to Eq. 4: [TNB] = 1.80 exp(-0.105*t*) -0.037*t* + 72.03. *Inset*: increasing concentrations of *Mt*AhpE were used (0.5 - 2.5 μM) and the amplitudes of the first phase (A) obtained from Eq. 4 were plotted against [*Mt*AhpE]. **B.** The slopes of the second phase (-S), obtained from the fit to Eq. 4, were plotted against A.

Figures

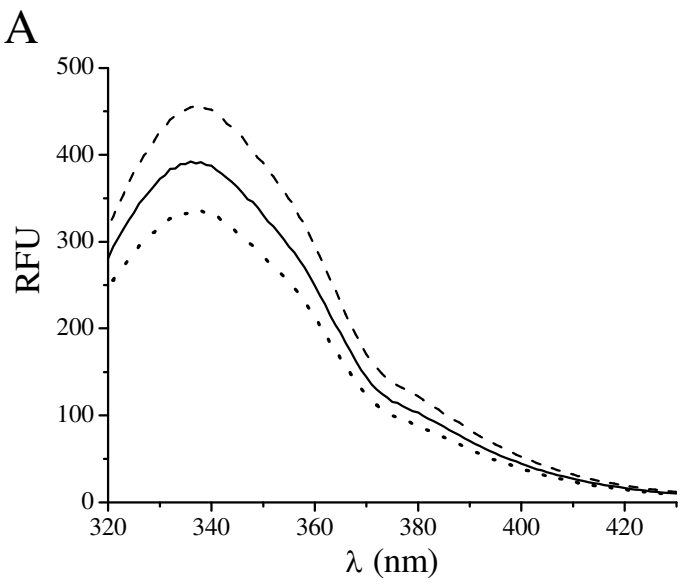

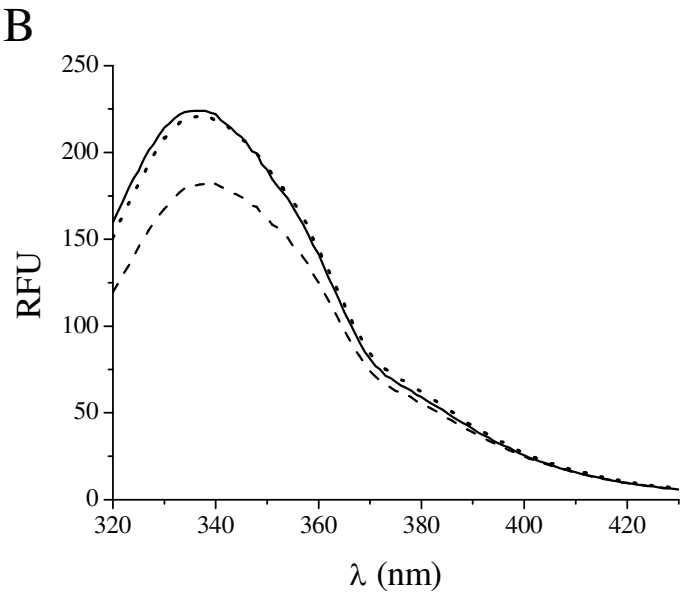

Hugo et al 2009, Figure 1

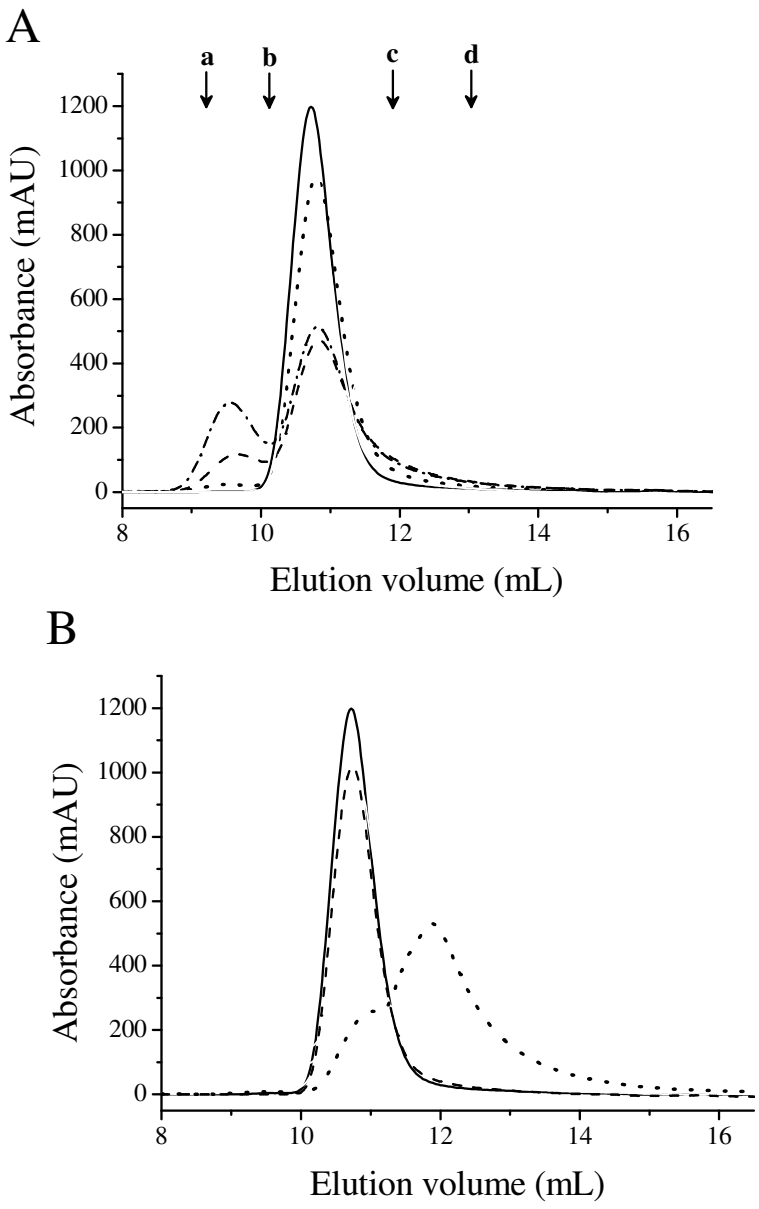
A
a
b
c
d
Absorbance (mAU)
Elution volume (mL)
B
Absorbance (mAU)
Elution volume (mL)

Hugo et al 2009, Figure 2

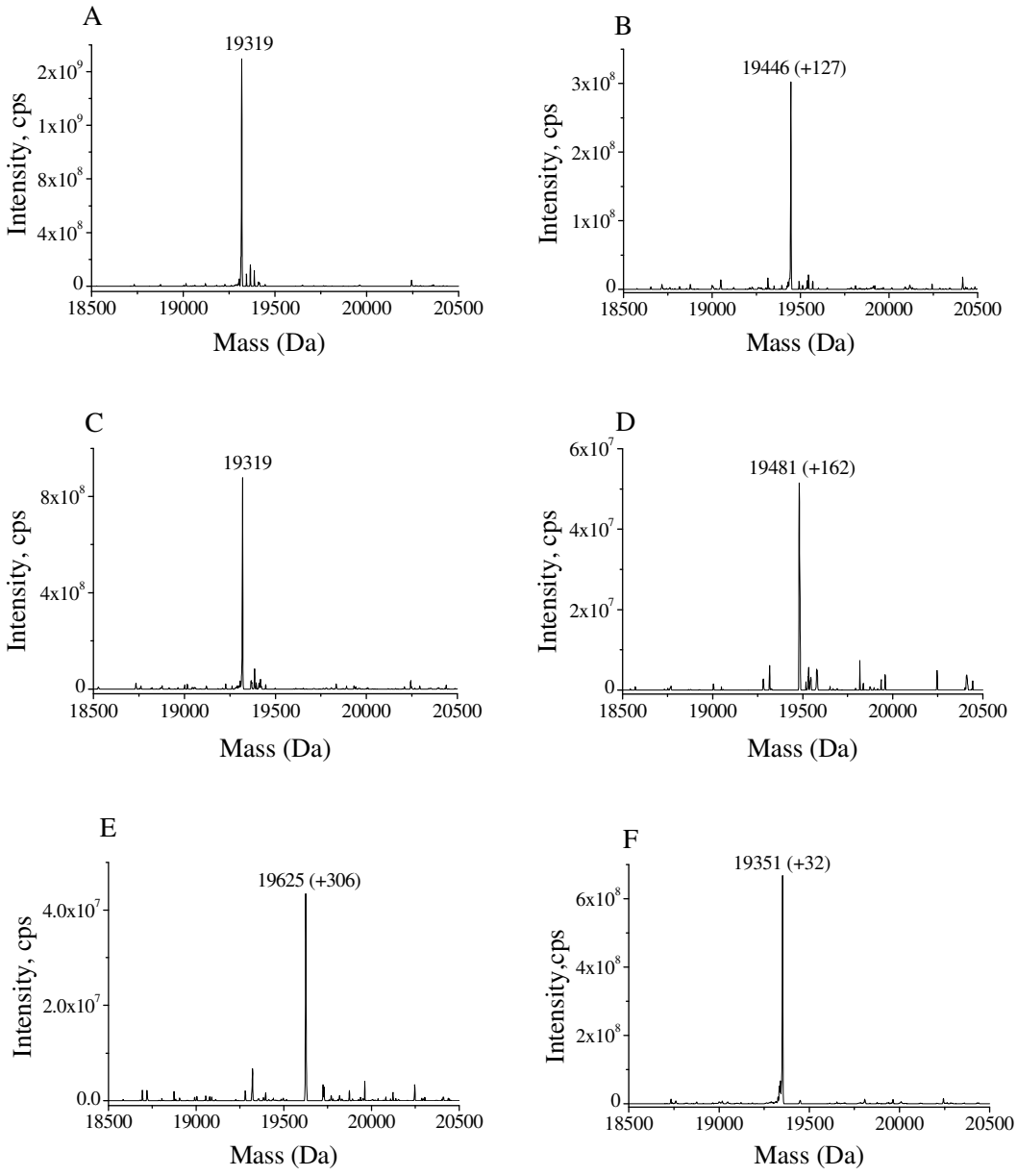

Hugo et al 2009, Figure 3

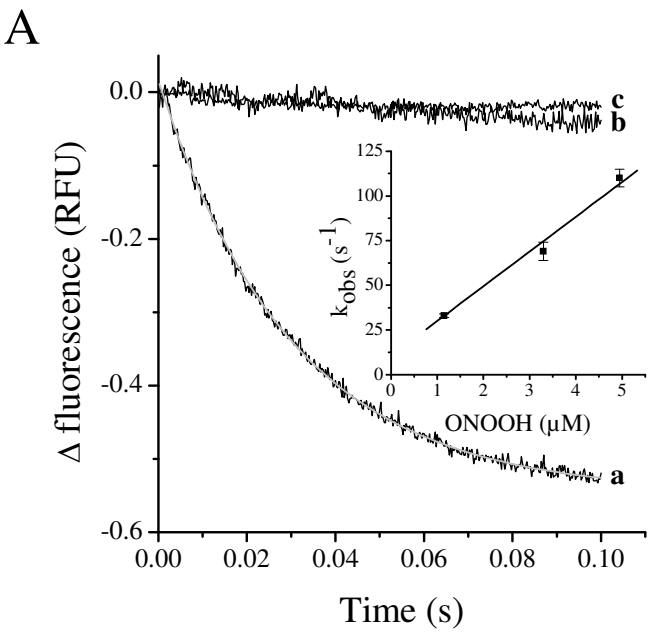

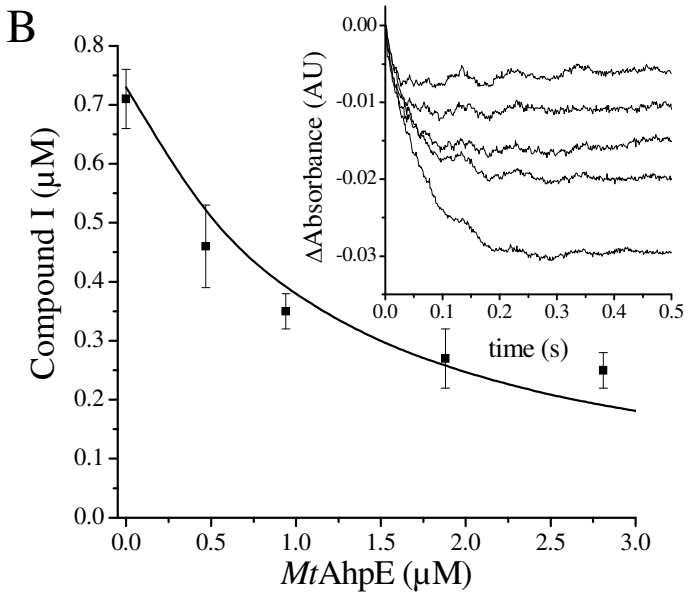

Hugo et al 2009, Figure 4

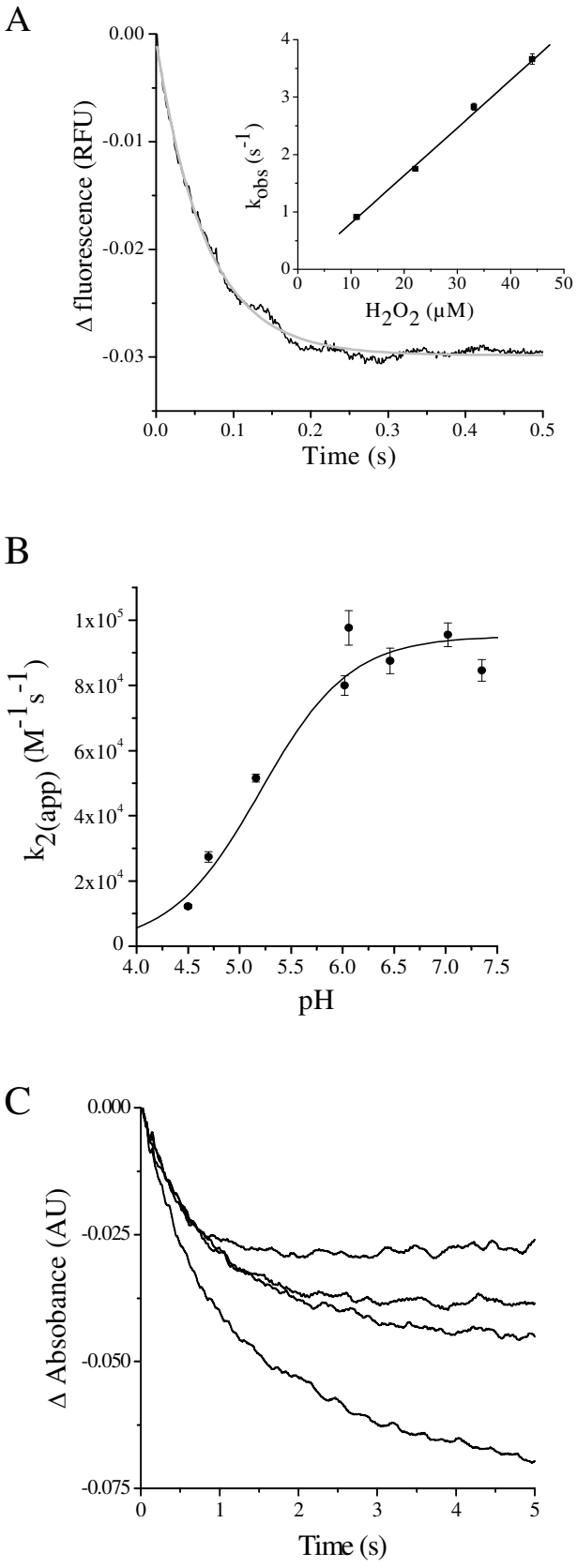

Hugo et al 2009, Figure 5

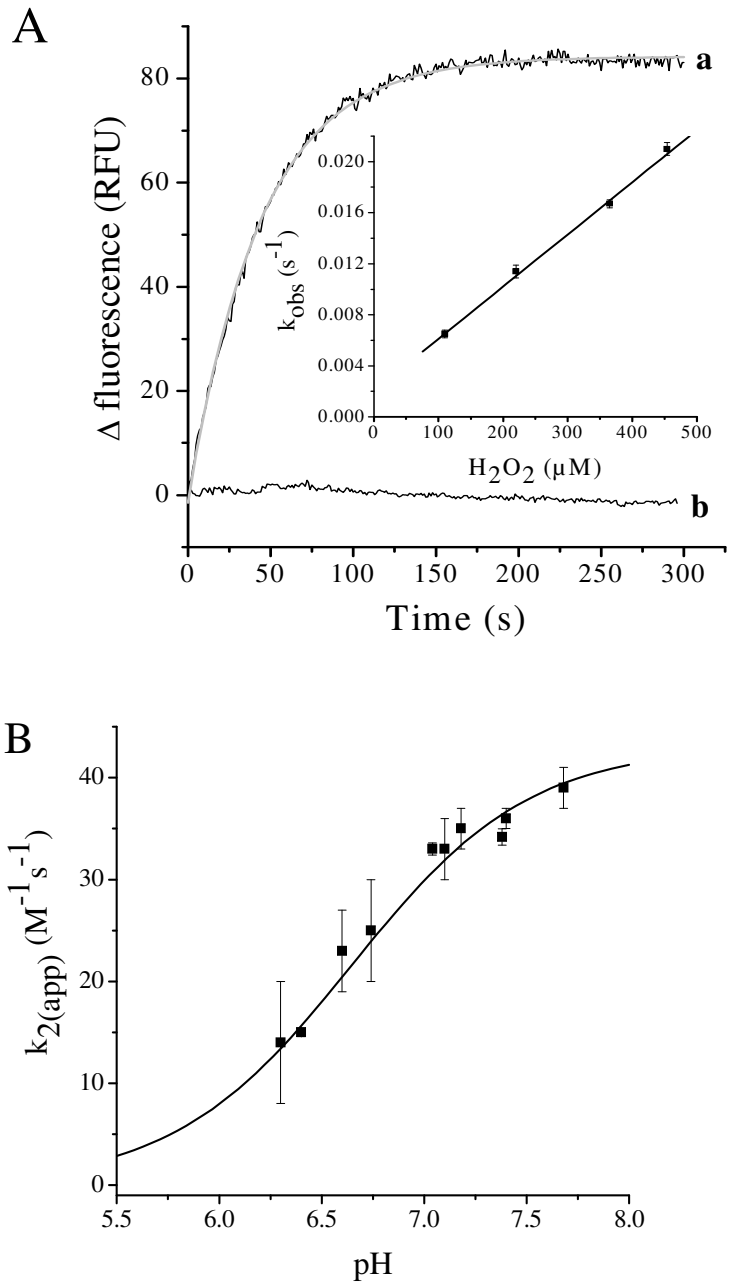

Hugo et al 2009, Figure 6

A

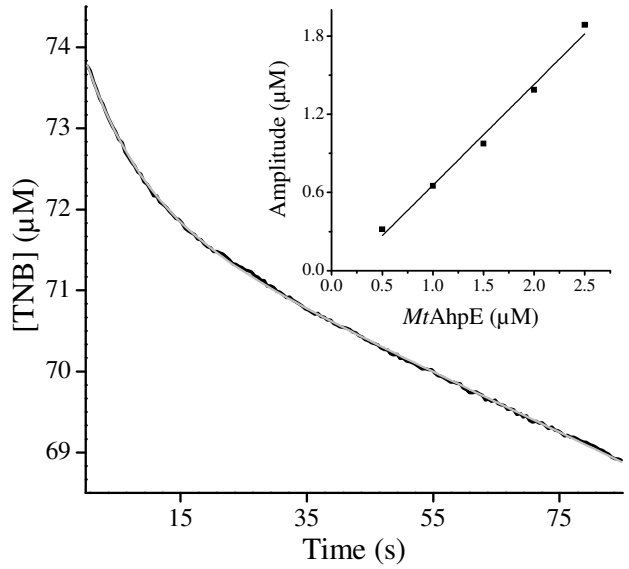

B

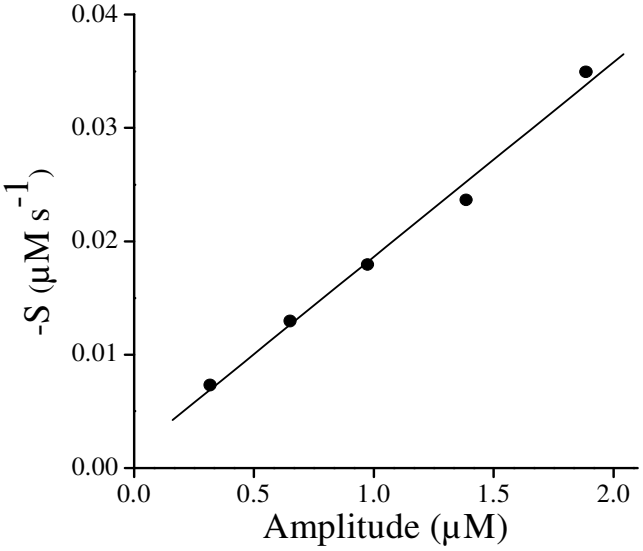

Hugo et al 2009, Figure 7

For Table of Contents Use Only

Thiol and sulfenic acid oxidation of AhpE, the one-cysteine peroxiredoxin from *Mycobacterium tuberculosis*: kinetics, acidity constants and conformational dynamics

Martín Hugo, Lucía Turell, Bruno Manta, Horacio Botti, Gisele Monteiro, Luis E. S. Netto, Beatriz Alvarez, Rafael Radi and Madia Trujillo